Source Model and Triggered Aseismic Faulting of the 2021 Mw 7.3 Maduo Earthquake Revealed by the UAV-Lidar/Photogrammetry, InSAR and Field Investigation

Ying-Hui Yang [1,2,*], Qiang Xu [1], Jyr-Ching Hu [3], Yun-Sheng Wang [1], Xiu-Jun Dong [1], Qiang Chen [4], Yi-Jun Zhang [4] and Hao-Liang Li [1]

[1] State Key Laboratory of Geohazard Prevention and Geoenvironment Protection, Chengdu University of Technology, Chengdu 610059, China
[2] Hebei Key Laboratory of Earthquake Dynamics, Sanhe 065201, China
[3] Department of Geosciences, National Taiwan University, Taipei 10617, Taiwan
[4] Department of Remote Sensing and Geoinformation Engineering, Southwest Jiaotong University, Chengdu 610031, China
* Correspondence: xzhfhyyy@126.com

Contents of this file

Introduction

Figure S1 shows the flowchart of the Lidar observation and data processing.

Figure S2 shows the estimated 3D surface deformation field of the 2021 Maduo earthquake.

Figure S3 Distinguished surface cracks along the seismogenic fault from UAV-Lidar DEM and optical images.

Figure S4 shows the destroyed Yematan and Changmahe bridges by the 2021 Maduo earthquake.

Figure S5 show the collapsed house of the Changmahe village in the southeast of seismogenic fault of the 2021 Maduo earthquake.

Figure S6 Aftershock distribution of the 2021 Mw 7.3 Maduo earthquake.

Table S1 shows the parameters of the InSAR pairs associated with the 2021 Maduo earthquake.

Table S2 shows the focal mechanisms of the historical earthquakes with magnitudes larger than M 6.0 and occurred 150 km within the East-Kunlun fault.

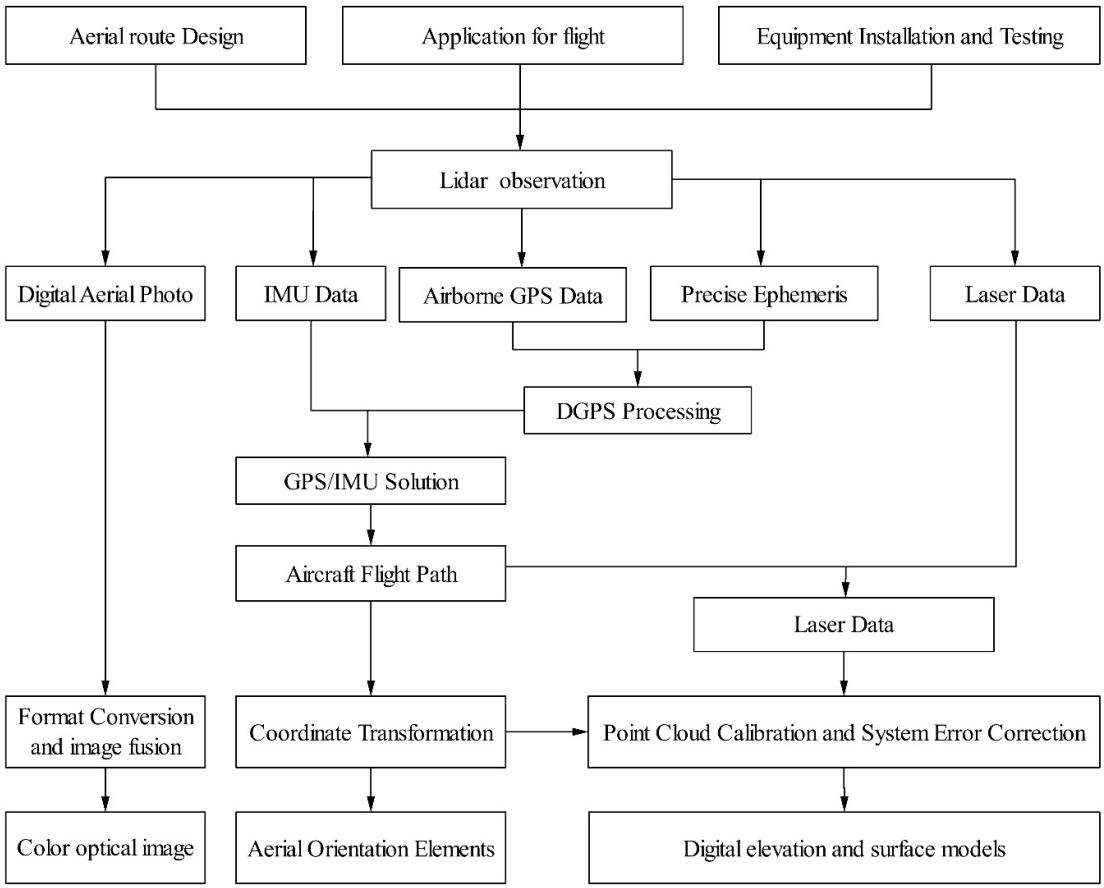

Figure S1. The flowchart of Lidar observation and data processing.

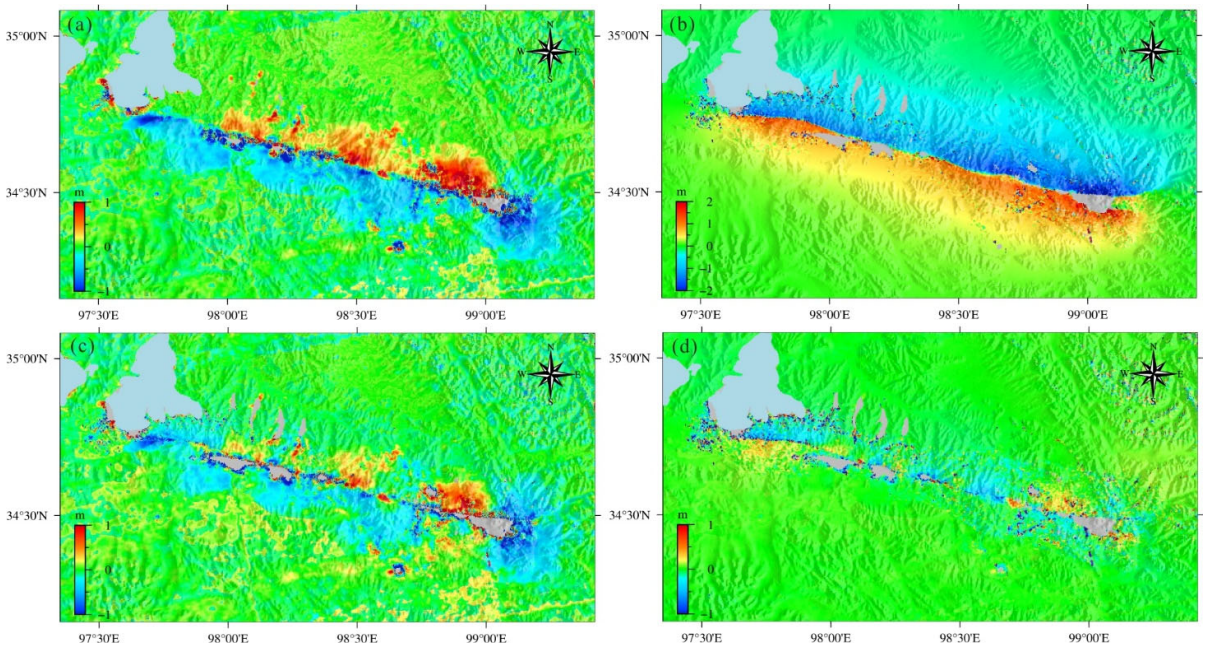

Figure S2. The estimated 3D surface deformation field of the 2021 Maduo earthquake. (a) Surface deformation along the azimuth direction of Sentinel-1 ascending track extracted based on the Multiple Aperture Interferometry (MAI) technique. (b) The estimated surface deformation along the east (b), north (c) and vertical (d) directions, respectively.

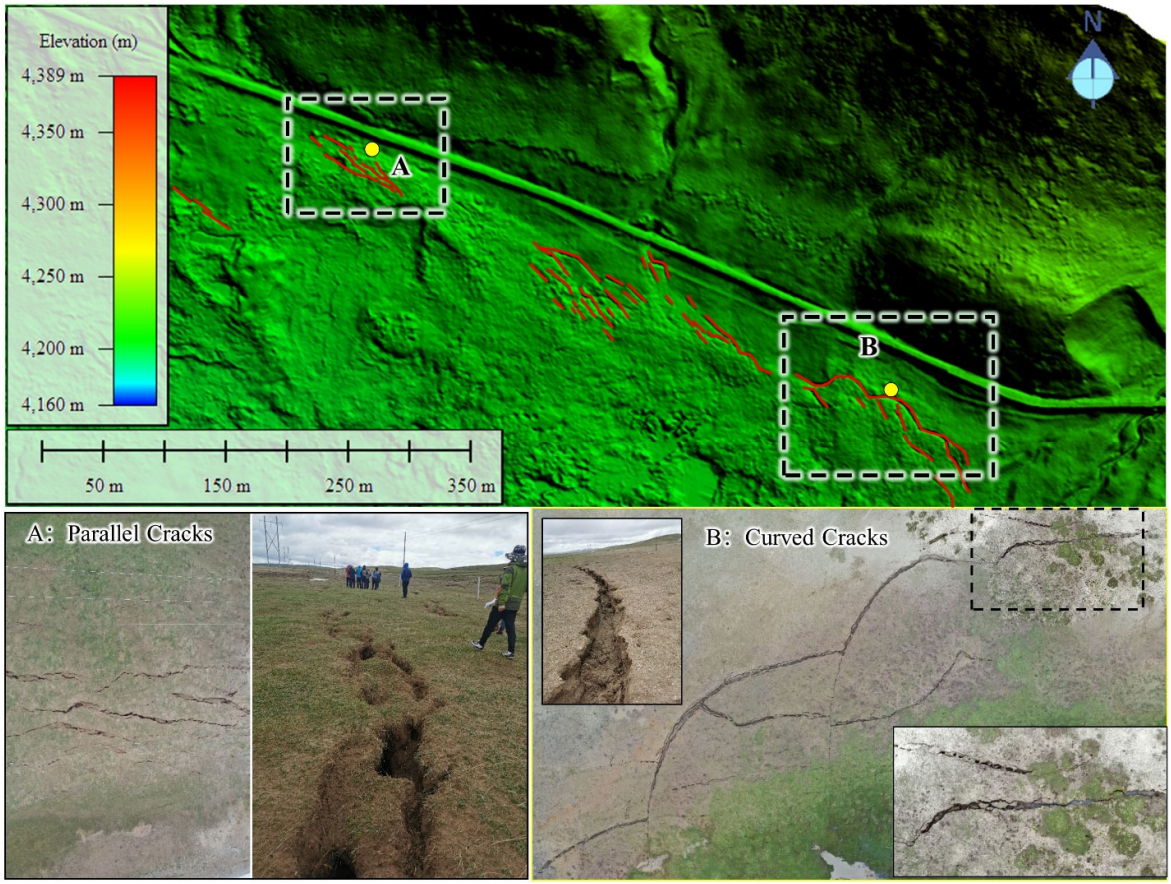

Figure S3. The distinguished surface cracks along the seismogenic fault from UAV-Lidar DEM and optical images.

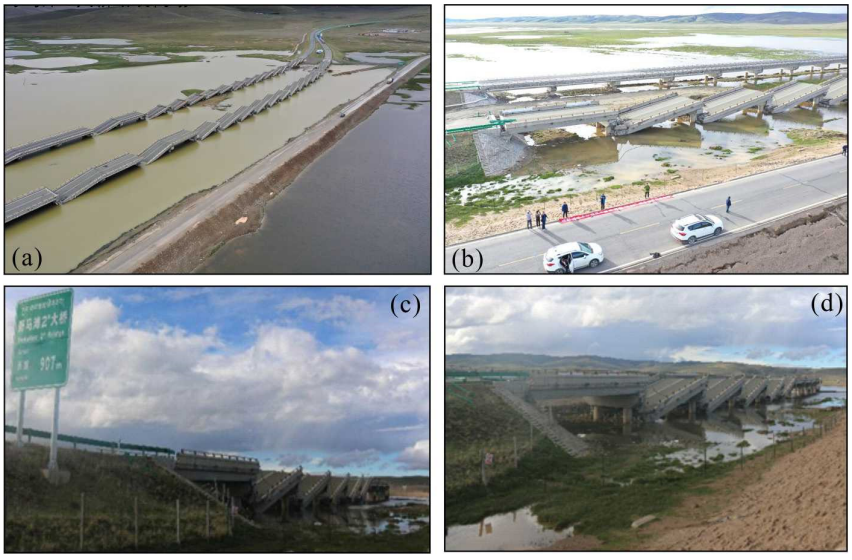

Figure S4. The destroyed Yematan (a-b) and Changmahe (c-d) bridges by the 2021 Maduo earthquake.

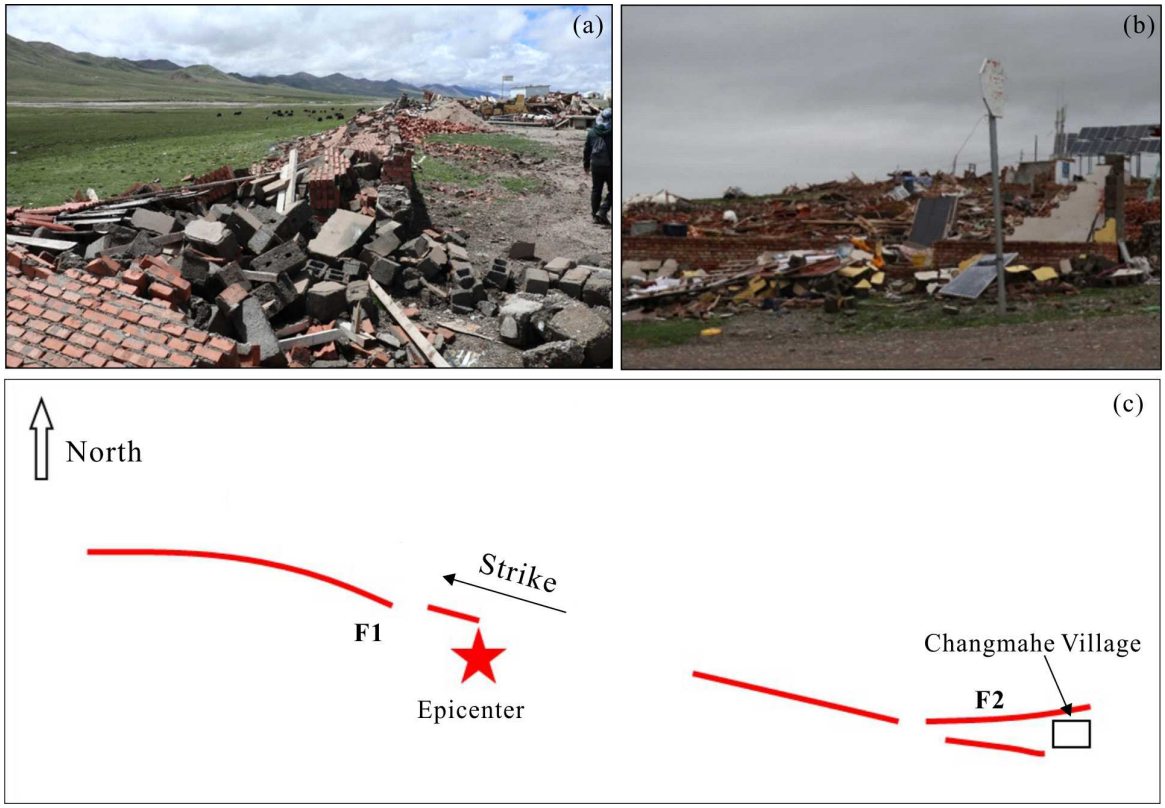

Figure S5. House collapse of the Changmahe village in the southeast of the seismogenic fault of the 2021 Maduo earthquake.

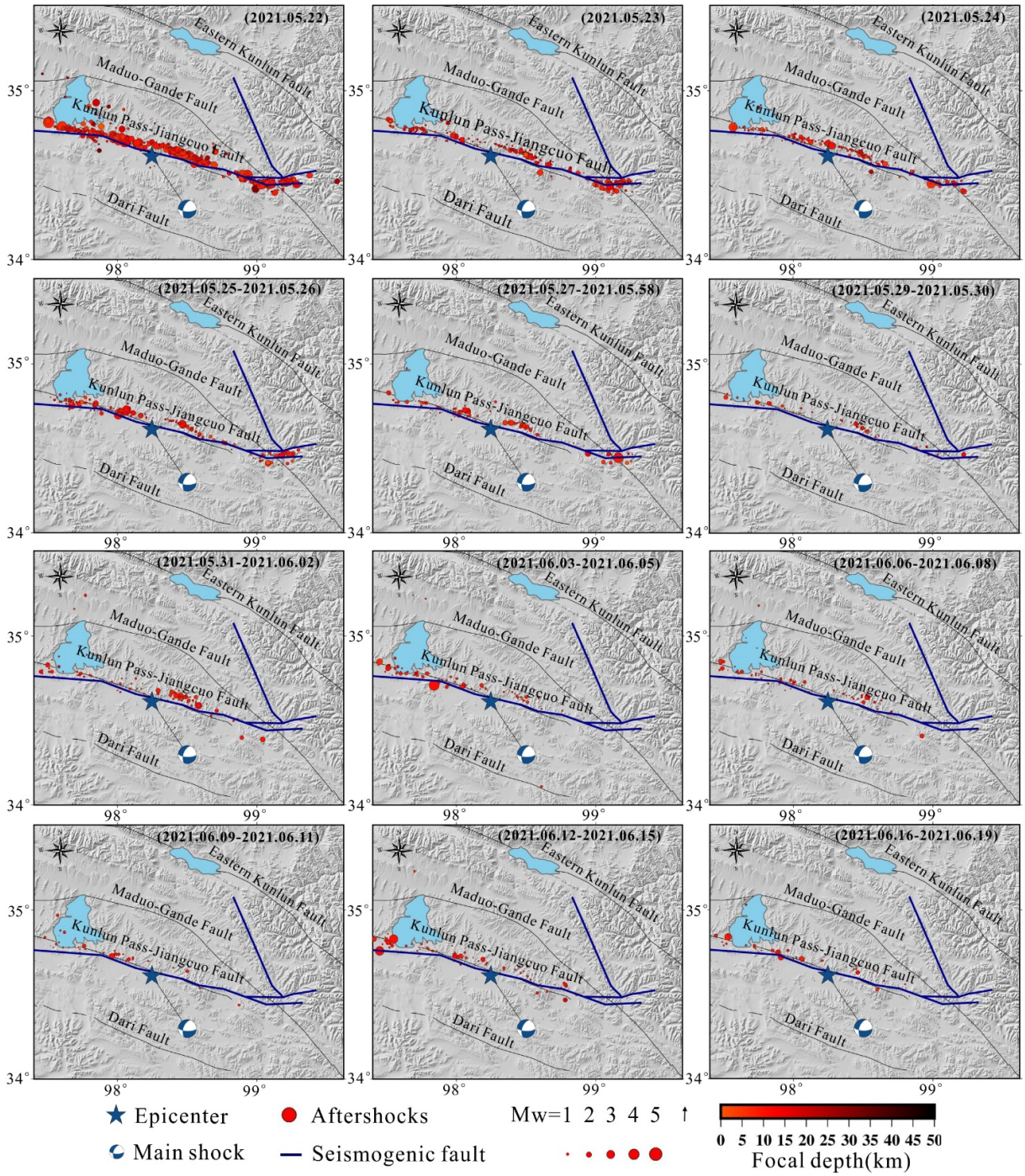

Figure S6. Aftershock distribution of the 2021 Mw 7.3 Maduo earthquake. Red circles denote the aftershocks after the mainshock, the blue lines indicate the co-seismic fault of the Maduo earthquake, the black liens show the surface trace of the fault around the seismic zone, the blue star indicates the epicenter of the Maduo earthquake.

Table S1. Parameters of the InSAR pairs associated with the 2021 Maduo earthquake.

Sensor	Orbit direction	Acquisition time	Heading angle (°)	Incidence angle (°)	Imaging mode
Sentinel-1	Ascending	2021/05/20-2021/06/19	-12.9	39.2	TOPS
Sentinel-1	Descending	2021/05/20-2021/06/13	-167.0	39.1	TOPS
ALOS-2	Descending	2021/02/04-2021/06/04	-170.0	39.0	ScanSAR

Table S2. Focal mechanism of the historical earthquakes with magnitude larger than M 6.0 and occurred 150 km within the East-Kunlun fault.

Time	Lon. (°)	Lat. (°)	Depth (km)	Magnitude (M)	Strike (°)	Dip (°)	Rake (°)
2017/08/08	103.855	33.193	9.0	6.5	153	84	-33
2001/11/14	90.541	35.946	10.0	7.8	97	89	-44
2000/09/12	99.343	35.389	10.0	6.3	343	80	-170
1990/04/26	100.254	36.239	9.6	6.3	101	46	41
1990/04/26	100.245	35.986	8.1	6.5	101	46	41
1990/04/26	100.332	36.047	10.0	6.2	101	46	41
1990/04/26	100.274	36.040	10.0	6.3	101	46	41
1963/04/19	96.440	35.530	20.0	6.7	277	80	-10
1947/03/17	99.500	33.300	15.0	7.3	135	60	60
1937/01/07	97.690	35.400	15.0	7.8	110	70	15